



Article

Spatio-Temporal Dynamic of Disturbances in Planted and Natural Forests for the Saihanba Region of China

Chienwei Tao ^{1,†}, Tong Guo ^{1,*,†} , Miaogen Shen ²  and Yanhong Tang ¹

¹ College of Urban and Environmental Sciences, and Key Laboratory for Earth Surface Processes of the Ministry of Education, Peking University, Beijing 100871, China; andrewtao@pku.org.cn (C.T.); tangyh@pku.edu.cn (Y.T.)

² State Key Laboratory of Earth Surface Processes and Resource Ecology, Faculty of Geographical Science, Beijing Normal University, Beijing 100875, China; shenmiaogen@bnu.edu.cn

* Correspondence: tongg@pku.edu.cn

† Co-first author.

Abstract: Various disturbances like extreme climate events, fires, and insect outbreak severely impact forest ecosystems, and differences are expected between planted and natural forests. However, there is little information on the spatio-temporal dynamics of the disturbances in terms of both forest types. In this study, we used the LandTrendr algorithm to detect disturbances in planted and natural forests in a temperate region of Northern China from 1985 to 2020 using Landsat and Sentinel 2 satellite data. The planted and natural forests suffered severe disturbances in 1994 in the south (park establishment) and in 2012 in the north (severe drought). More than one third of the area of planted (37.5%) or natural (35.8%) forests was highly disturbed. The duration of forest disturbances was mostly 1 to 3 years in terms of planted or natural forests. The NDVI anomaly of the planted forests decreased from 0.24 to -0.08 after drought events, while the reduction was from 0.22 to -0.06 for natural forests. Afterwards, the NDVI anomaly of the planted forests showed a slow upward variation but not for the natural forests. This study allows us to evaluate the response of various forest types to disturbance regimes.

Keywords: classification; drought; NDVI; time series; temperate forest



Citation: Tao, C.; Guo, T.; Shen, M.; Tang, Y. Spatio-Temporal Dynamic of Disturbances in Planted and Natural Forests for the Saihanba Region of China. *Remote Sens.* **2023**, *15*, 4776. <https://doi.org/10.3390/rs15194776>

Academic Editor: Henning Buddenbaum

Received: 29 August 2023

Revised: 22 September 2023

Accepted: 28 September 2023

Published: 30 September 2023



Copyright: © 2023 by the authors. Licensee MDPI, Basel, Switzerland. This article is an open access article distributed under the terms and conditions of the Creative Commons Attribution (CC BY) license (<https://creativecommons.org/licenses/by/4.0/>).

1. Introduction

Forest ecosystems cover one third of the global terrestrial area [1], and contribute 50% of the net primary production of terrestrial ecosystems [2]. Forest ecosystems suffer from an increasing intensity or frequency of disturbances such as droughts, fires, and insect outbreaks in many regions of the world [3]. Disturbances were classically defined as discrete events that disrupt the community by changing the space, food resources and the physical environment [4]. Forest disturbances severely impact the structure and functions of forest ecosystems [3]. It is estimated that the disturbances led to a loss of 2.3 million km² of natural forest area during the period from 2000 to 2012 [5]. The changes in forest structure and composition, in turn, feedback on the dynamics of forest disturbances [6]. Climate change and forest management exacerbated forest disturbances [7,8]. The influencing degree and underlying mechanisms vary greatly with disturbance types [9], e.g., forest composition and age structure differ considerably between clearcutting-origin stands and fire-origin stands [10]. In addition, the effects of forest disturbances on ecosystem functioning and biodiversity differ considerably across various spatio-temporal scales [11]. Thus, mapping the spatio-temporal patterns of forest disturbances is the first step in understanding the impact of the disturbance. Recent studies have carried out a large amount of work concerning this issue, with studies conducted in North America [12,13], Europe [14], and China [15]. In recent decades, the disturbance type present in Canada was characterized by insects, while the United States of America and Mexico mostly suffered disturbances in terms of

forest harvesting [13]. The frequency of forest disturbance increased while the disturbance strength decreased in Europe [14]. Forest disturbances showed a decreasing trend in China owing to forest protection policies [15]. However, large-scale disturbance dynamics usually ignore the heterogeneity of background environmental conditions compared to that at a small spatial scale, e.g., a specific forest region. More importantly, forest ecosystems are composed of various types of forests, and the variety determines how the structure and functioning of the forest ecosystems change with an increasing intensity and frequency of disturbances [16,17]. However, a quantitative evaluation of disturbance dynamics was scarce for different types of forests, e.g., natural forests and planted forests.

The area of planted forests has shown a rapidly increasing trend, but that of natural forests has decreased globally since 1990 [1]. Planted forests account for 36% of the total forested area in China [18]. However, the negative effects of planted forests on ecological processes have received significant attention [19]. Land resources are rather limited in China. Thus, evaluating the spatio-temporal dynamic of disturbances for both forest types helps forest managers to optimize land use plans. The effects of disturbances on both forest types should not be neglected. On the one hand, planted forests are mainly composed of a relatively tree species. On the other hand, natural forests are characterized by diverse tree species [20]. This leads to many differences in terms of response between both forest types to disturbances, e.g., drought [21–23]. On the other hand, planted forests often have high water demand and thus decrease the water available to natural forests [24]. Planted forests are usually characterized by high planting density, and this exacerbates the effects of drought and thus impacts the ecosystem functioning of forests, especially in water-limited regions [25]. In addition, studies of disturbances on planted forests should be strengthened in water-limited or cold areas as these areas are characterized by a relatively slow recovery rate in terms of vegetation after disturbances. Further understanding the responses of both forest types to drought is closely associated with mitigating the effects of climate change.

This study examined the spatio-temporal dynamics of disturbances in natural and planted forests in the Saihanba region of China. Moreover, we specified the response of both forest types to drought disturbances.

2. Materials and Methods

2.1. Overview of the Methods

We collected multi-source satellite data and performed various pretreatments to control the data quality. We then trained a random forest classifier to determine the distribution of the planted and natural forests in the study area. After that, we detected forest disturbances through the use of the LandTrendr algorithm based on the index Normalized Burn ratio (NBR) and examined the spatio-temporal dynamic of the disturbances for both forest types. We specifically quantified drought disturbances through the standardized precipitation evapotranspiration index (SPEI); further, we analyzed their impact on the growth of both forest types using the index NDVI anomaly. An overview of the method is given in Figure 1.

2.2. Study Area

This study selected natural and planted forests located in Saihanba National Forest Park (116°32'~118°14'E, 41°35'~42°40'N) in the Hebei Province of China (Figure 2). The park is located in the temperate continental monsoon climate zone. The area of study site is 933.33 km². The duration of winter is long, up to 230–240 days per year. The frost-free period is short. The temperature difference between day and night is large. The potential evapotranspiration is usually more than the annual precipitation. There are many types of climate hazards such as strong winds, sandstorms, droughts and frost. Based on the weather record from 1960 to 2015, the mean annual temperature is −1.5 °C, and the extreme daily low temperature is −43.3 °C. The mean annual precipitation is 452.6 mm. The altitude of the study area ranges from 1100 m to 1950 m. The average value is 1500 m. The altitude distribution of planted forests is higher than that of the natural forests. The dominant tree species in natural forests are *Larix principis-rupprechtii*, *Picea asperata* Mast and *Betula*

platyphylla Suk. The planted forests are characterized by *Pinus sylvestris* var. *mongolica* and *Larix principis-rupprechtii*. The Saihanba region is a very important part of the Three-North Forest Shelterbelt Project in China. As of 2020, the forest area is 767.4 km² and the forest coverage is 82%.

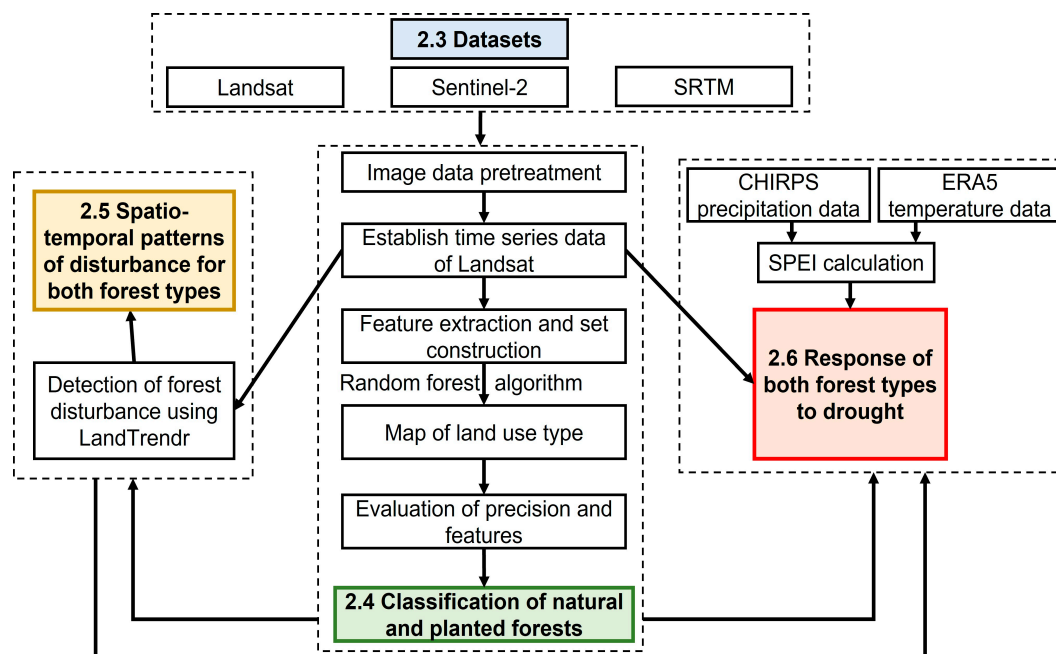


Figure 1. The conceptual scheme of this study. Each black dashed box corresponds to Sections 2.3–2.6, as follows.

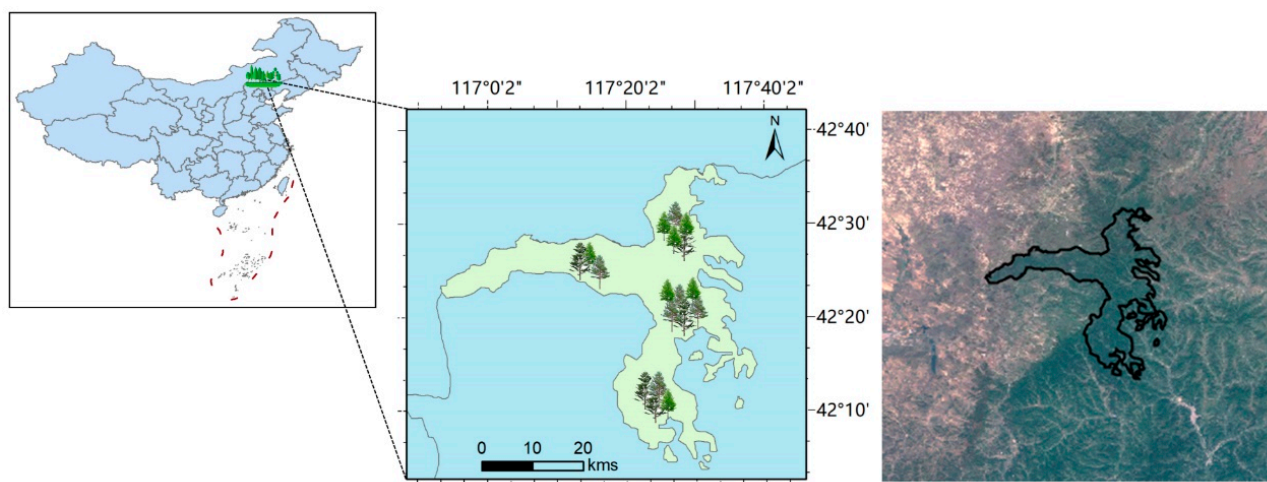


Figure 2. The location and Sentinel-2 remote sensing image of Saihanba Region in China.

2.3. Datasets

The satellite datasets included the land surface reflectance products from Landsat 5, Landsat 7 [26], Landsat 8 [27] and Sentinel-2 [28] (Tables 1 and 2). The reflectance data at Blue, Green, Red, NIR, SWIR 1, SWIR 2 and Cirrus bands used in this study have a spatial resolution of 30 m and a temporal resolution of 16 days, covering the period from 1985 to 2020 (Table 3). The spatial and temporal resolutions of the Sentinel-2 reflectance at the same bands with Landsat 8 in 2020 are generated to 30 m and 5 days, respectively. The Landsat 8 and the Sentinel-2 were used to conduct land use type classification in 2020. Simultaneously, we carried out field surveys in the research area in August 2020 and in July

2021. We selected several representative sites and identified the planted and natural forests of these sites. Landsat 5, Landsat 7 and Landsat 8 were used to analyze the long-term dynamics of the forest disturbances. Data collection and pretreatment were conducted on the cloud platform of the Google Earth Engine (GEE) [29,30]. We classified land use types and evaluated the disturbance dynamic for planted and natural forests on GEE. For the classification, we collected image data from Sentinel-2 and Landsat 8 in the year 2020. For the evaluation, we obtained data for different time periods from Landsat 5, Landsat 7 and Landsat 8 from GEE. The pretreatment aimed to remove clouds and enable image synthesis. These treatments were also conducted on GEE. The cloud was filtered by its percentage in a pixel grid of the Sentinel-2 image. The Landsat image applied the CFMask algorithm for cloud removal.

Table 1. Products of Landsat satellite and used bands.

Satellite	Landsat 5		Landsat 7		Landsat 8	
Sensor	TM		ETM+		OLI	
	Band	Wavelength (μm)	Band	Wavelength (μm)	Band	Wavelength (μm)
Parameters of bands	Blue	0.40–0.52	Blue	0.45–0.52	Coastal	0.43–0.45
	Green	0.52–0.60	Green	0.52–0.60	Blue	0.45–0.51
	Red	0.63–0.69	Red	0.63–0.69	Green	0.53–0.59
	NIR	0.76–0.90	NIR	0.76–0.90	Red	0.64–0.67
	MIR	1.55–1.75	MIR	1.55–1.75	NIR	0.85–0.88
	MIR	2.08–2.35	MIR	2.08–2.35	MIR	1.57–1.65
	TIR	10.40–12.50	TIR	10.40–12.50	MIR	2.11–2.29
			PAN	0.52–0.90	PAN	0.50–0.68
					IRC	1.36–1.38
					TIR	10.60–11.19
				TIR	11.50–12.51	

Note: NIR denotes near-infrared; MIR denotes mid-infrared; TIR denotes thermal infrared; PAN denotes panchromatic; IRC denotes infrared cirrus.

Table 2. Products of Sentinel-2 satellite and used bands.

Satellite	Sentinel-2A		Sentinel-2B	
Sensor	MSI			
	Band	Center Wavelength (μm)	Band	Center Wavelength (μm)
Parameters of bands	Coastal	0.44	Coastal	0.44
	Blue	0.50	Blue	0.49
	Green	0.56	Green	0.56
	Red	0.66	Red	0.67
	RE	0.70	RE	0.70
	RE	0.74	RE	0.74
	RE	0.78	RE	0.78
	RE	0.86	RE	0.86
	NIR	0.84	NIR	0.83
	WV	0.95	WV	0.94
	SWIR	1.37	SWIR	1.38
	SWIR	1.61	SWIR	1.61
	SWIR	2.20	SWIR	2.19

Note: RE denotes red edge; NIR denotes near-infrared; WV denotes water vapor; SWIR denotes short-wave infrared.

Table 3. Information concerning datasets.

Data	Satellite						Weather	
	Landsat 5	Landsat 7	Landsat 8	Sentinel-2A	Sentinel-2B	CHIRPS	ERA5-Land	
Spatial resolution (m)	30	30	30	30 *	30 *	5566	27,830	
Source of acquisition	GEE	GEE	GEE	GEE	GEE	GEE	GEE	
Time period	1 January 1985– 31 December 2011	1 January 1999– 31 December 2018	1 January 2013– 31 December 2020	1 May 2020– 30 September 2020		1 January 1985– 31 December 2020		

Note: “*” means that the spatial resolution is 10 m for original Sentinel-2 collection. To match Landsat collection data, we regenerated Sentinel-2 data to a 30 m spatial resolution.

We used the standardized precipitation evapotranspiration index (SPEI) to quantitatively mirror drought disturbances [31]. The index can determine the onset, duration, and strength of drought events. The index is based on a three-month moving average and was calculated using precipitation and temperature data. The precipitation data are taken from the dataset of Climate Hazards Group InfraRed Precipitation with Station data (CHIRPS) with a spatial resolution of 0.5° and a temporal resolution of one day. The dataset is often used to detect precipitation extremes and long-term precipitation changes [32]. The temperature data are taken from the dataset of ERA5-Land with a spatial resolution of 0.1° and a temporal resolution of one hour [33]. We used the air temperature of 2 m above the ground surface. Precipitation and temperature data were obtained from GEE. There are 83 pixels from the CHIRPS dataset falling into the study area. There are 5 points from the ERA5-Land dataset located in the study site. The temperature data were input into the Thornthwaite function to calculate potential evapotranspiration. The SPEI index was obtained through the logistic fitting of the probability density function constrained by the time series data of the difference between precipitation and potential evapotranspiration. We used average values to integrate data of different spatio-temporal resolutions.

2.4. Classification of Natural and Planted Forests

Evaluating the spatio-temporal variations of the disturbances in natural and planted forests first needs a precise classification of forest types. Satellite data are very effective in terms of examine forest ecosystems [34] and have been successfully applied to the classification of natural or planted forests [35–37]. We trained a random forest classifier to determine the spatial distribution of planted and natural forests in the Saihanba region. The labels of planted and natural forests for training the random forest classifier were selected via field survey, and information taken from the topographic map were selected through a visual interpretation of the high-resolution image slices from GEE. We used spectral features, texture, and terrain factors to obtain the characteristics of different ground objects and then train the classifier (Table 4). Vegetation has specific spectral features. Green plants can absorb visible light via their chlorophyll and reflect near-infrared light. In addition, the composition of planted forests is relatively singular compared to natural forests. That is, the spectrum of planted forests tends to have a more regular distribution. The texture features were achieved using the Gray-level Co-occurrence Matrix [38]. The terrain factors, like slope, elevation, and hill shade, were accounted for using the Shuttle Radar Topography Mission (SRTM) database [39]. We also calculated different indices to accurately differentiate ground objects. The indices include NDVI [40] (Equation (1)), normalized difference water index (NDWI) [41] (Equation (2)) and normalized difference built-up (NDBI) [42] (Equation (3)). The number of training points for different ground objects is given in Table 4. Kappa coefficient in the confusion matrix was used to assess the accuracy of the classification. Specifically, the coefficient compares the consistency between reference samples and classification samples [43]. The time period of the classification was determined from 1 May to 30 September 2020 to minimize the noise of ice and snow. We used the same classification mask across the study time period (1985–2020). To accurately

distinguish planted and natural forests, we also conducted field investigations in August 2020 and July 2021. It should be noted that we did not classify specific tree species in natural or planted forests. The samples of the classification were randomly divided into two groups (70% and 30%) using a bootstrap approach. In this study, 70% of the samples were used to train the classifier and 30% were used for validation.

$$NDVI = \frac{NIR - R}{NIR + R} \quad (1)$$

$$NDWI = \frac{NIR - MIR}{NIR + MIR} \quad (2)$$

$$NDBI = \frac{SWIR - NIR}{SWIR + NIR} \quad (3)$$

where NIR denotes the reflectance of the near-infrared band; R denotes the reflectance of the red band; MIR denotes the reflectance of the mid-infrared band; and SWIR denotes the reflectance of the short-wave infrared band.

Table 4. The number of training points for different ground objects.

Ground Objects	The Number of Training Points
Natural forests	480
Planted forests	652
Building	175
Water	102
Grassland	184
Agriculture Land	236
Bare Land	134

2.5. Spatio-Temporal Pattern of Disturbance

We evaluated the spatio-temporal patterns of natural and planted forest disturbances based on the surface reflectance products of Landsat 5, Landsat 7, and Landsat 8 during the period from 1985 to 2020. We performed multi-band matching between Landsat 5, Landsat 7 and Landsat 8 on GEE. We selected three months (1 June to 31 August) of the growing season to extract the satellite images, and then defined, matched, and transformed the spectral reflectance of various sensors from three Landsat satellites. We used the median of three months and LandTrendr (Landsat-based Detection of Trends in Disturbance and Recovery) algorithm to detect long-term forest disturbances [44]. The algorithm is dependent on high-quality image synthesis and it is insensitive to interannual signal noise. The core idea of the algorithm is time series segmentation and is used to detect whether forest disturbances have occurred by evaluating the pixel's spectral time series. Specifically, the segmentation based on the LandTrendr algorithm is conducted with an annual time step [45]. The maximum number of segments in this study was set to 6; segment number was then detected using the algorithm for the time series data. The algorithm takes a single point of view from a pixel's Normalized Burn ratio (NBR), identifies breakpoints, separating time periods of durable change, and eventually records the year that the disturbances occurred. Specifically, the year of disturbance was determined based on the varying magnitude of the transition between segments. The variation corresponds to the largest decrease for the time series data of NBR. To increase the reliability of disturbance detection, the minimum observation was set to 11 pixels. A single disturbance area is assumed to be greater than this value (approximately 1 km² in reality). We used the index of NBR to evaluate the strength of forest disturbances. The index was calculated based on Equation (4). The index has been proven to be very sensitive to disturbances [46,47]. Moreover, the accuracy of the index was found to be higher than other indices like NDVI and normalized difference moisture index (NDMI) regarding disturbance detection [48]. Thus, the index is deemed as a proxy for forest disturbances. We divided the forest disturbances into various levels based on

changes in the NBR index. Values less than 0.2 are defined as being not or slightly disturbed. Values between 0.2 and 0.5 are defined as moderately disturbed. Values between 0.5 and 0.8 are defined as highly disturbed; that is, the study area suffers a total loss of forests.

$$NBR = \frac{NIR - SWIR}{NIR + SWIR} \quad (4)$$

where NIR denotes the reflectance of the near-infrared band, and SWIR denotes the reflectance of the short-wave infrared band.

2.6. The Response of Natural and Planted Forest to Drought

The SPEI index usually indicates the meteorological degree of drought degree in a region [49]. The index has been widely used in research focusing on assessing meteorological drought conditions [50,51]. We classified the drought degree into different levels based on the value of the index: $SPEI \geq -0.5$: no drought; $-1.0 < SPEI \leq -0.5$: slight drought; $-1.5 < SPEI \leq -1.0$: moderate drought; and $SPEI \leq -1.5$: heavy drought. We thereafter calculated the three-month moving average value of SPEI, which was widely used to monitor vegetation response to drought [52]. The calculation of the index was performed using the ‘SPEI’ package in R software [53].

We extracted monthly NDVI time series data based on the mask of the spatial distribution of planted and natural forests. The NDVI data were then filtered using the Savitzky–Golay method [54]. This method can weaken the negative effects of weather conditions and data quality on the time series data, keeping the time series data relatively stationary. We executed the method using the package ‘spatialEco’ in R software. To better evaluate the response of vegetation to drought, we calculated the index of NDVI anomaly (Equation (5)). The value of the index being more than 0 indicates no disturbance, while less than zero indicates various degrees of disturbance. Specifically, the value of mean NDVI corresponds to a normal level of vegetation growth. Less than zero implies poor vegetation growth conditions; that is, the vegetation is at risk of disturbances.

$$NDVI_{anomaly} = (NDVI_i - NDVI_{mean}) / NDVI_{\sigma} \quad (5)$$

where $NDVI_{anomaly}$ denotes the value of NDVI in month i of the target year; $NDVI_{mean}$ denotes the mean of NDVI in month i from the years 1985 to 2020; and $NDVI_{\sigma}$ denotes the standard deviation of NDVI in month i from the years 1985 to 2020.

We used Spearman’s correlation analysis to examine the relationship between SPEI and NDVI anomaly of planted and natural forests. In addition, we applied generalized additive models to fit the temporal dynamics of NDVI anomaly of planted and natural forests within three years after drought events to better understand the ecological effects of drought. It should be noted that we did not consider the interactive effects of different drought disturbances on the growth of both forest types. That is, individual drought disturbances were deemed independent events. We assume that decreased changes in both forest types after drought events correspond to forest resistance to drought disturbances, while increased changes correspond to recovery processes after drought disturbances. All statistical analyses were performed using R software.

3. Results

3.1. Distribution of Natural and Planted Forests

The spatio resolution of land use type classification was 30 m (Figure 3a). The overall accuracy of the classification was 93.9% (Table 5). The value of the Kappa coefficient was 0.92 in terms of identifying planted and natural forests. The planted forests were mainly distributed in the northwest of the Saihanba region, while natural forests grew in the southeastern part (Figure 3b). The area of natural and planted forests was 58,509 km² and 48,594 km², respectively.

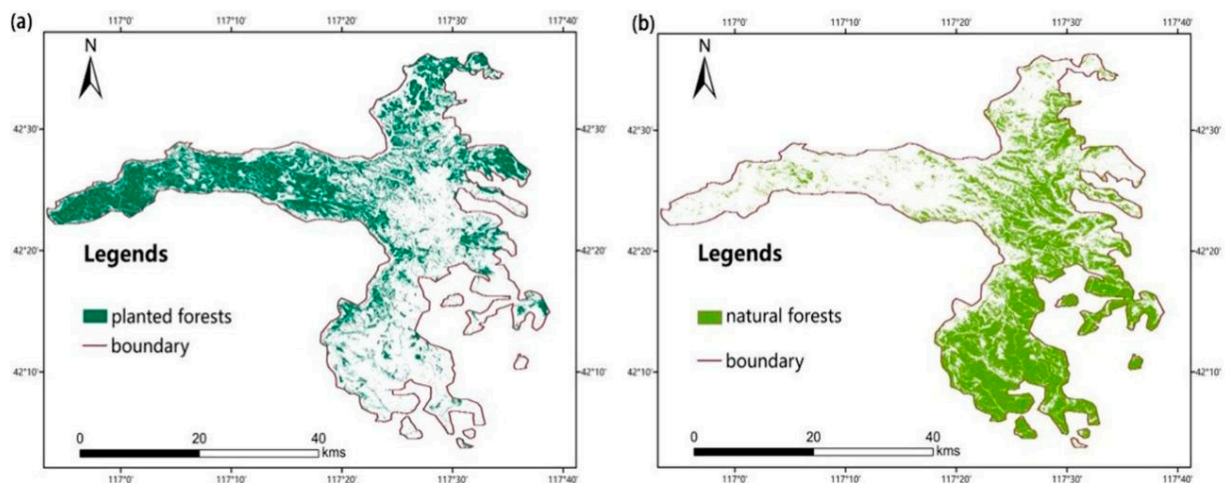


Figure 3. Spatial distribution of planted (a) and natural (b) forests in the Saihanba region of 2020.

Table 5. The classification accuracy of land use types in the study area.

Land Use Types	Producer's Accuracy (%)	User's Accuracy(%)
Planted forest	91.0	93.8
Natural forest	92.3	93.5
Building	97.9	97.9
Water	100	100
Grassland	95.4	87.3
Agriculture land	98.5	94.1
Bare land	97.2	100
Overall accuracy (%)	93.9	
Kappa coefficient	0.92	

3.2. Spatio-Temporal Patterns of Forest Disturbances

Forest disturbances mostly occurred in two time periods, namely, from 1991 to 1998 and from 2007 to 2014 (Figure 4a,b). In addition, the number of forest disturbances had great inter-annual variations. Specifically, the area of forest disturbances occurring in 1994 and 2012 was far greater than that of other years. In 1994, disturbances occurred in south Saihanba (Figure 4b). The disturbance area proportion (4%) of natural forests was larger than that (0.5%) of planted forests (Figure 5). In contrast, forest disturbances were mostly distributed in north Saihanba in 2012 (Figure 4a). The disturbance area proportion of planted (2.5%) and natural (2%) forests was approximately the same.

More than one-third of the area of planted (37.5%) or natural (35.8%) forests was highly disturbed. About 60% of forest disturbances were of lower intensity regardless of planted or natural forests (Figure 6a,b). High-intensity disturbances in natural forests occurred in the south of Saihanba, with a denser spatial distribution than that for planted forests in the north. The duration of forest disturbances was mostly 1 to 3 years in terms of planted or natural forests (Figure 6c,d).

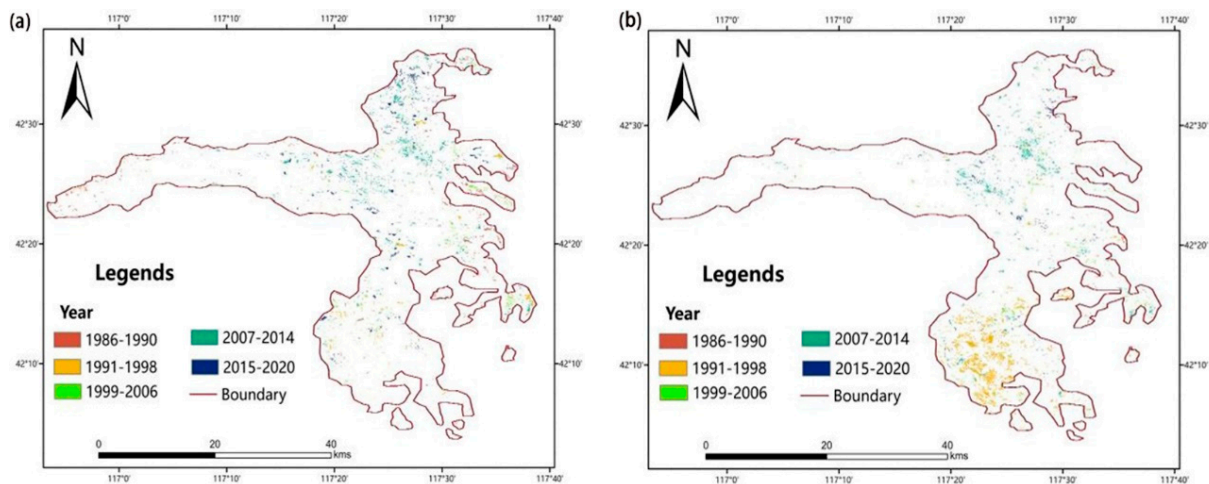


Figure 4. Spatial distribution of disturbances in planted (a) and natural (b) forests during the period from 1985 to 2020 in the Saihanba region.

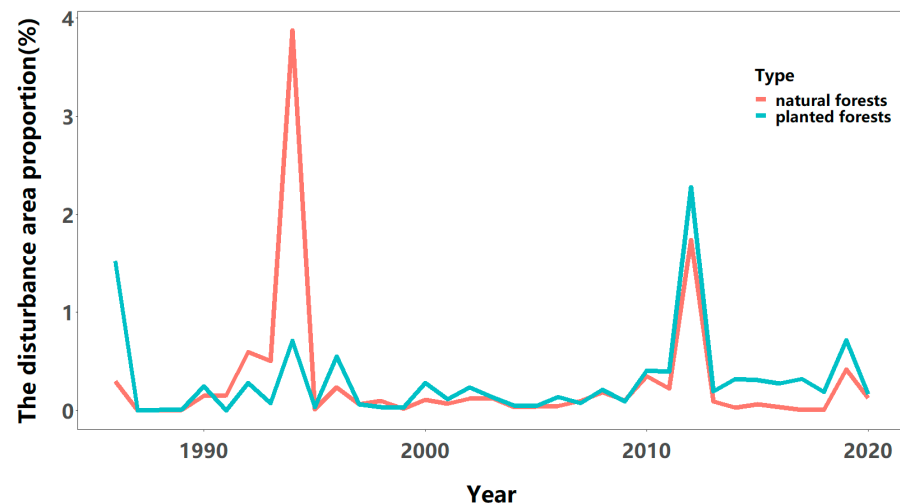


Figure 5. The disturbance area proportion of planted and natural forests during the period from 1985 to 2020.

3.3. The Response of Planted and Natural Forests to Drought

The time period from 1985 to 2020 witnessed 50 moderate drought events and 23 heavy drought events (Figure 7). Specifically, two heavy drought events occurred in December 1998 and April 1994, respectively, before 2000. In contrast, there were 21 heavy drought events after 2000. The index of NDVI anomaly of both planted and natural forests had a significantly negative correlation with the index of SPEI. However, the correlation was not strong for either planted forests ($R = -0.31$) or natural forests ($R = -0.34$).

The NDVI anomaly of planted forests showed a faster decreasing rate than that of natural forests in the previous year and was half of that after drought disturbances (Figure 8a). Specifically, the NDVI anomaly of the planted forests changed from 0.24 to -0.08 , while the variation changed from 0.22 to -0.06 for natural forests. After that period, the NDVI anomaly of planted forests presented a slow upward variation, while the NDVI anomaly of natural forests kept a relatively consistent level. In terms of heavy drought events, neither planted forests nor natural forests experienced recovery within three years after the disturbance of heavy drought (Figure 8b). Moreover, the decreasing rate of NDVI anomaly for planted forests was slightly higher than that of natural forests.

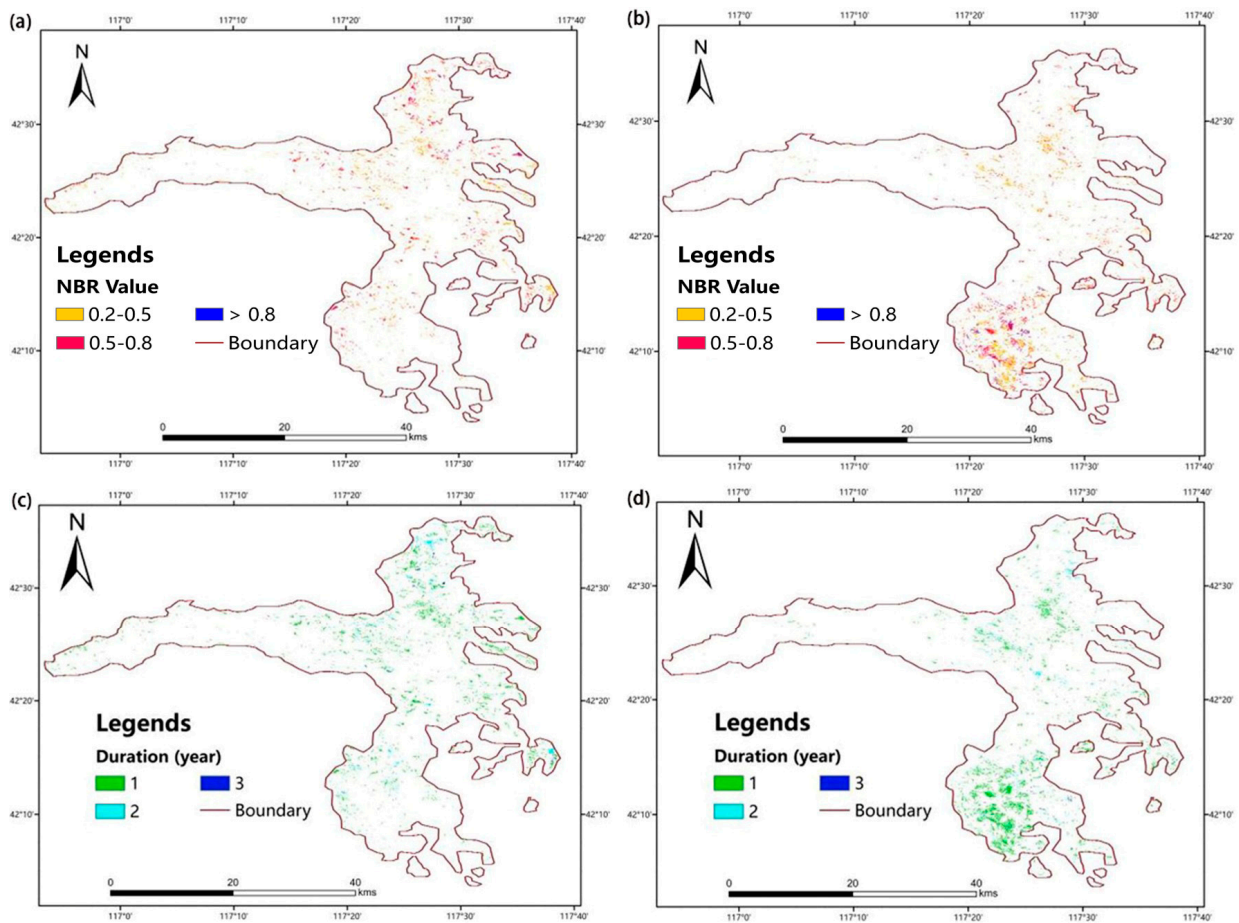


Figure 6. Spatial distribution of forests disturbance strength ((a): planted; (b): natural) and intervals ((c): planted; (d): natural) based on 36 years of integrated data from the Saihanba region.

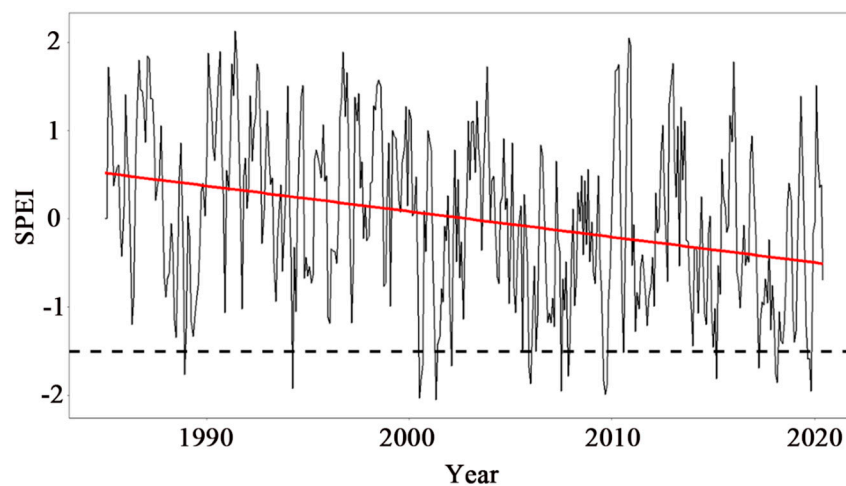


Figure 7. Time series of SPEI during the period from 1985 to 2020 in the Saihanba region.

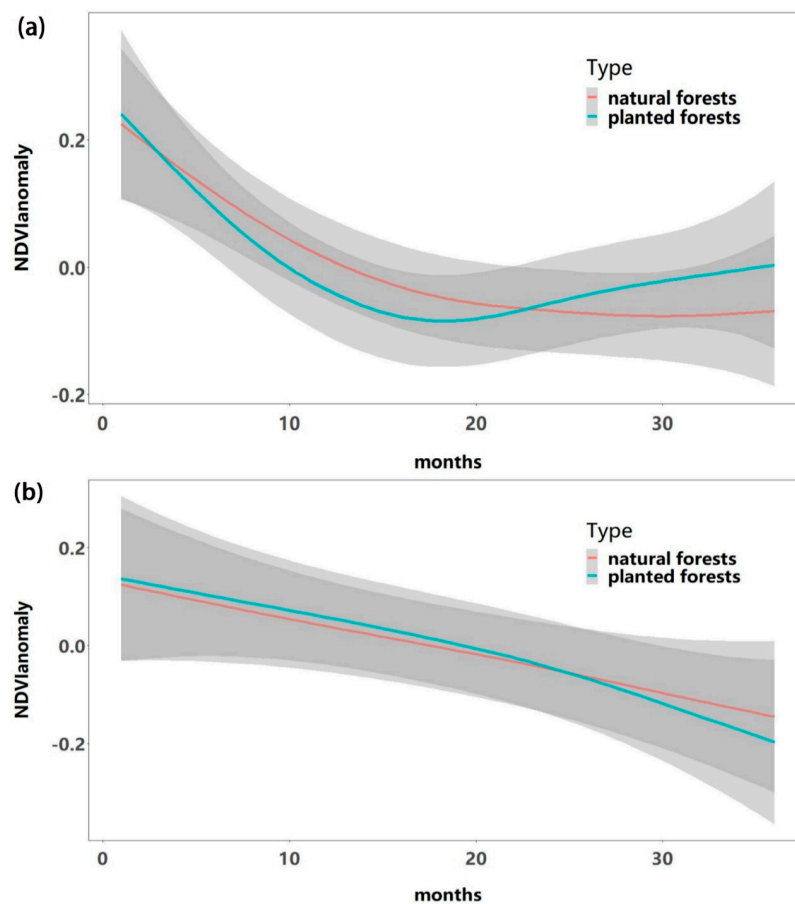


Figure 8. Changes in the index of NDVI anomaly after all drought events (a) and heavy drought events (b) for planted and natural forests. The value of zero on the x-axis indicates the occurring year of drought disturbances. The solid lines denote mean values of NDVI anomaly. The gray shadows denote standard deviation of NDVI anomaly.

4. Discussion

4.1. Classification of Planted and Natural Forests

Separating planted forests from other vegetation types is rather challenging [37]. We only considered adult planted forests for the forest type classification since young planted forests present very similar values in terms of NDVI compared with grass. The main species of planted forests include *Larix* and *Pinus sylvestris*. The age of these adult planted forests ranges from 40 to 60. Natural forests have a similar age range compared with planted forests. Additionally, the times series data obtained are very short for young planted forests. According to local plantation records, it is supposed that the adult forests identified in 2020 were already matured trees in 1985. The matured trees are dependent on age. In addition, in light of local climatic and vegetation characteristics, the possibility of natural forests converting to other land use types was very small during the period from 1985 to 2020. However, it is possible that natural forests or grasslands have been converted to planted forests owing to human activities. To improve the accuracy of forest type classification, we accounted for various geographical factors, as the plantation of planted forests is largely constrained by elevation and slope. The elevation of the Saihanba region gradually decreases from north to south. Regional afforestation was first performed in the north and west. We handled the satellite data of growing seasons since phenological differences between both forest types in the growing seasons are more sensitive to capture than in the other seasons [35]. Natural forests are more diversely structured than planted forests [55]. This will lead to more mixed pixels in natural forests. Differences in environ-

mental conditions like soil nutrients and soil moisture may also impact the accuracy of forest type classification.

4.2. Spatio-Temporal Dynamic of Disturbances in Planted and Natural Forests

The high-intensity disturbance in the year 1994 may be related to the establishment of the Saihanba National Forest Park. The park was established in 1993 [56]. Especially in the early stage of its establishment, forests were severely destroyed due to the construction of infrastructure, roads, parking lots and service facilities. Moreover, the planted forests in the Saihanba region are mostly located in the north, while the natural forests are in the south. The forest park is also located in the south of the Saihanba region. This leads to highly intensive disturbance signal in the south of the year 1994. The severe drought possibly explained the high-intensity disturbance of the year 2012. Since the density of trees was found to be closely related to drought intensity and frequency in the Saihanba region [57], we examined precipitation records during the period from 1985 to 2020 in the Saihanba region and found that the annual precipitation was very sparse in 2011. In detail, ten months of this year were meteorologically defined as drought months. Further, the result showed no distinct long-term trend in the disturbance area proportion of both forest types. At national or regional scales, the rate of forest disturbances markedly decreased owing to protection policies between 1986 and 2020 in China. The magnitude and frequency of the disturbances have weakened in Northeast China [15]. In Europe, a proportion of 17% of forests suffered disturbances, with an increasing frequency and a decreasing strength during the time period from 1986 to 2016 [14]. On the global scale, forest disturbances are likely to increase with elevations in temperature [3]. We found that the natural forests were disturbed in a spatially dense way while sparsely for the planted forests. This suggests that the natural forests are susceptible to disturbances. Planted forests with greater management probably avoid some disturbances because human activities (e.g., irrigation and tree species selection) can reduce negative effects in terms of disturbances [58]. Parts of the planted forests suffered short-duration and highly intensive disturbances. On the one hand, this could be attributed to large-scale reforestation. On the other hand, planted forests may suffer multiple disturbance events like high-frequency wood collection from forest farms. For highly disturbed areas, forests may have been converted to other land use types like grassland, bare land, and agricultural or construction land. For moderately disturbed areas, forests may suffer disturbances like intermediate cutting, droughts, insect outbreaks, fires, etc. The aggregation of various disturbance types can exacerbate ecological effects in terms of vegetation dynamics. Moreover, vegetation loss induced by these disturbances conversely feeds back to the spatio-temporal dynamics of forest disturbances [3]. Elevation may also impact the dynamics of the disturbances for both forest types. At lower elevations, the disturbance area of natural forests was larger than that of planted forests. While the opposite trend was true at higher elevations (Figure A3). This is mostly dependent on the distribution of both forest types along the gradient of elevation.

4.3. Response of Planted and Natural Forests Vary with the Intensity of Drought Disturbance

The index of NDVI anomaly has been proven to be a sensitive probe to detect the effects of drought on vegetation changes [59]. We found that drought disturbances were characterized by a large inter-annual variation and a very low spatial heterogeneity in the Saihanba region. In addition, the area of natural forests was a little larger than that of planted forests. This means that natural forests have a higher probability of suffering from drought than planted forests. Vegetation is assumed to not rapidly respond to drought disturbances; that is, drought disturbances have legacy effects on the vegetation dynamics of forest ecosystems [60]. Thus, we set a monitoring period of three years. We found that planted forests experienced a faster decreasing rate but a stronger recovery than the natural forests when we examined the ecological effects of all drought events. This finding is consistent with a study conducted on the national scale [55]. The natural forests are assumed to have higher species richness, diverse age stages and more complex community

structures than the planted forests [61]. In addition, natural forests are less water-consuming than planted forests in China [62]. However, Luo et al. [23] found that natural forests are more vulnerable to drought than planted forests. We further found that the shape of the response curve for both forest types was much similar with the results taken for summer (see Figure 3a). This suggests that the growth state in growing seasons played a key role in modulating forest response to drought. In addition, the resistance and recovery processes of both forest types were rather different across the four seasons. Different tree species are diversely sensitive to drought events of each season [63]. Our results indicated that damaged forests could not recover after heavy drought events regardless of planted or natural forests. The biomass of tropical forests in Africa and America showed a rapidly decreasing trend but no recovery after extreme drought [64]. This finding also hints at a hydraulic threshold for the response of tree growth to drought disturbances [65,66]. In cases where the disturbance intensity exceeds the recovery edge of trees, this may lead to the collapse of the forest ecosystem. Thus, we should be aware of different types of extreme climate events in the process of forest management.

4.4. Limitations and Perspectives

The data quality of the Landsat remote sensing images was poor in the early stages. This may reduce the detection accuracy of disturbances in planted and natural forests owing to the loss of data in some regions. MODIS-Landsat multi-source data can be used to establish relatively complete and less polluted times series data. This will minimize the influence of image data itself on the evaluation of forest dynamics. The image data samples used to classify planted and natural forests were partly constrained by the validation owing to the lack of detailed local forest inventory data. The classification mask of the year 2020 was used across the study time period since the resolution of earlier images was not as satisfactory as those taken in 2020. Even though we referred to graphs of local forest planning, spatio-temporal errors were not avoidable. We used the LandTrendr algorithm to capture spatio-temporal variations in forest disturbances. The advantage of the algorithm is the fact that it is less computationally intensive. However, there are few recorded materials to verify the results of forest disturbances obtained using the algorithm. The algorithm is based on pixel-by-pixel calculation and does not involve the spatial relationships between pixels. It only provides years of disturbance and cannot indicate the seasonal dynamics of the disturbance, like the continuous change detection and classification (CCDC) algorithm. The number of segments in the LandTrendr algorithm should be increased to capture multiple disturbances over a long time period [45]. Spatial distribution was graphed for the number of segments detected in every pixel of planted and natural forests (Figure A5). The value of segments is 1 for undisturbed pixels and 2 to 6 for disturbed pixels. Larger values of segments indicate more frequent disturbances in terms of pixels. The number of segments can partly mirror multiple disturbances in terms of pixels in the study area. The problem of overfitting may exist during the process of algorithm execution. These partly impact the evaluation of the long-term dynamics of forest disturbances. In addition, the algorithm can not separate individual disturbance types like drought, fire, insect outbreak, deforestation, etc., for characterizing the spatio-temporal dynamics of forest disturbances. It is very important to identify which disturbance type dominantly drives the forest dynamics for local forest management. The reliability of NDVI anomaly is largely constrained by the quantity and quality of images. The index SPEI usually indicates meteorological drought conditions at a large spatial scale. Although we compared pixels falling into the study area in terms of meteorological data and found that differences between pixels were not obvious, there may also exist heterogeneity in terms of micro-climate conditions at smaller spatial scales. During the study period, vegetation constantly exists after drought disturbances, even heavy drought events, for both forest types. However, we should be aware that the index NDVI anomaly is not sensitive to disturbances for totally destroyed forests where disturbances still occurred. The mechanisms underlying the response of planted and natural forests to drought need to be further studied. Since trees are vulnerable to scarce

precipitation in arid and semi-arid ecosystems [67], these ecosystems need a long time for the restoration of damaged forests. We did not explicitly consider the independent and compounding effects of individual drought events. Subsequent or multiple droughts have been found to increase the vulnerability of forests, especially for gymnosperms and conifer-dominated ecosystems [68]. In addition, forest age, density and specific species also determine drought sensitivity and recovery of planted and natural forests [22,69]. Forest growth is jointly determined by these factors, which need to be further studied.

5. Conclusions

Afforestation and reforestation efforts are still ongoing, and the area of planted forests is increasing in China. Climate extremes and interference of human activities are expected to increase under the background of global warming. These partly exacerbate forest disturbances. The basic assumption is that there exist differences in the disturbance dynamics between planted and natural forests. On the one hand, the intensity and frequency of forest disturbances varied with time and space. On the other hand, the planted forests experienced a faster decreasing rate but a stronger recovery than that of natural forests after drought events. These results are highly beneficial for local forest management and are very helpful to answer fundamental questions concerning afforestation and reforestation like “Which area is more suitable for plantation of trees” and “Which forest type suits better with local environmental conditions”.

Author Contributions: Conceptualization, Y.T. and T.G.; Data analysis, C.T.; Writing, original draft preparation, T.G.; Writing, review and editing, M.S.; visualization, C.T.; project administration, Y.T. All authors have read and agreed to the published version of the manuscript.

Funding: This research was funded by the National Key Research and Development Program of China, grant number 2019YFA0606602.

Data Availability Statement: Not applicable.

Acknowledgments: This work was supported by the National Key Research and Development Program of China (No.2019YFA0606602).

Conflicts of Interest: The authors declare no conflict of interest.

Appendix A

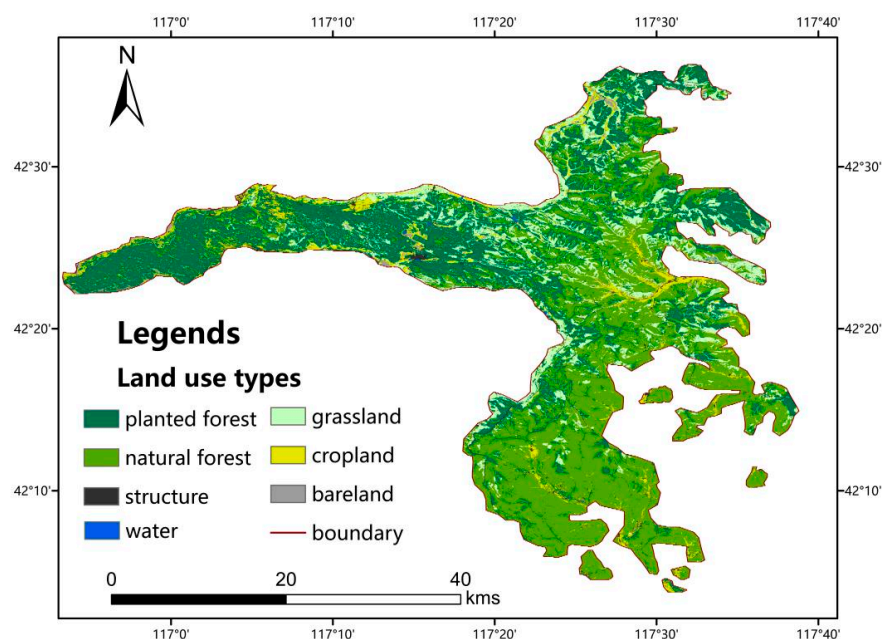


Figure A1. Classification of land use types in the Saihanba region in 2020.

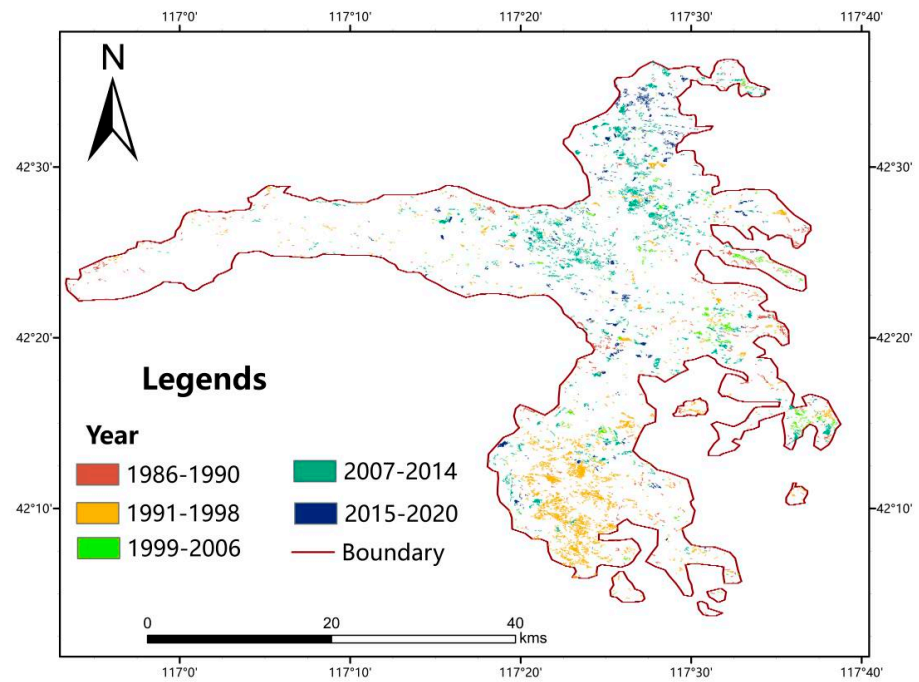


Figure A2. Spatial distribution of forest disturbances during the period from 1986 to 2020 in the Saihanba region.

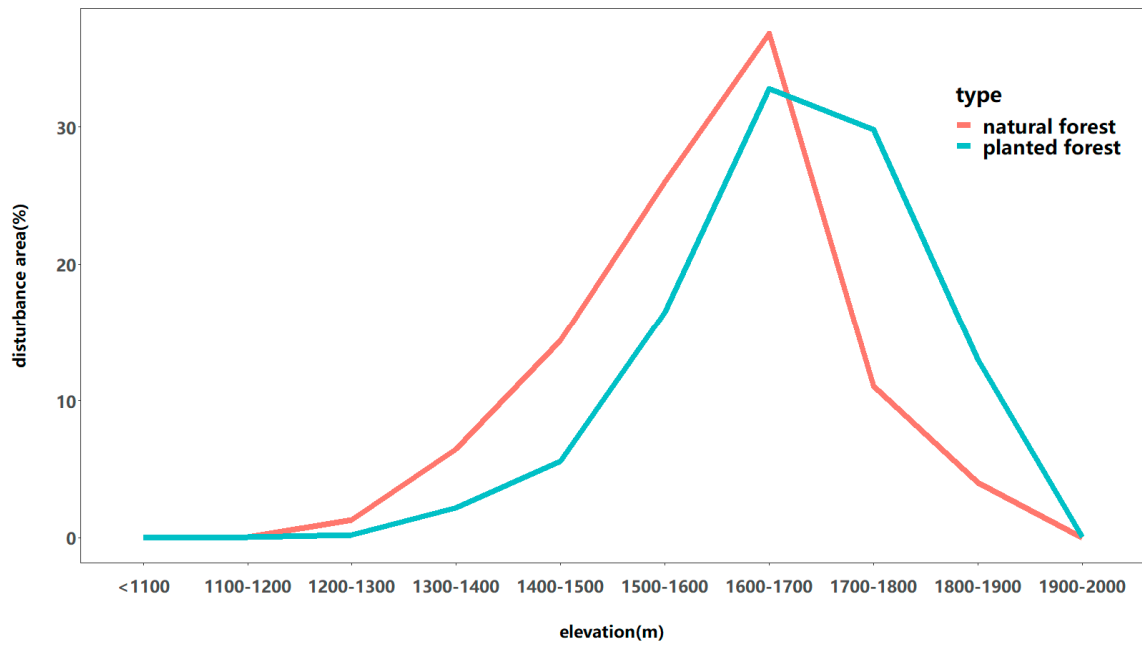


Figure A3. Proportion of disturbance area along the gradient of elevation for natural and planted forests.

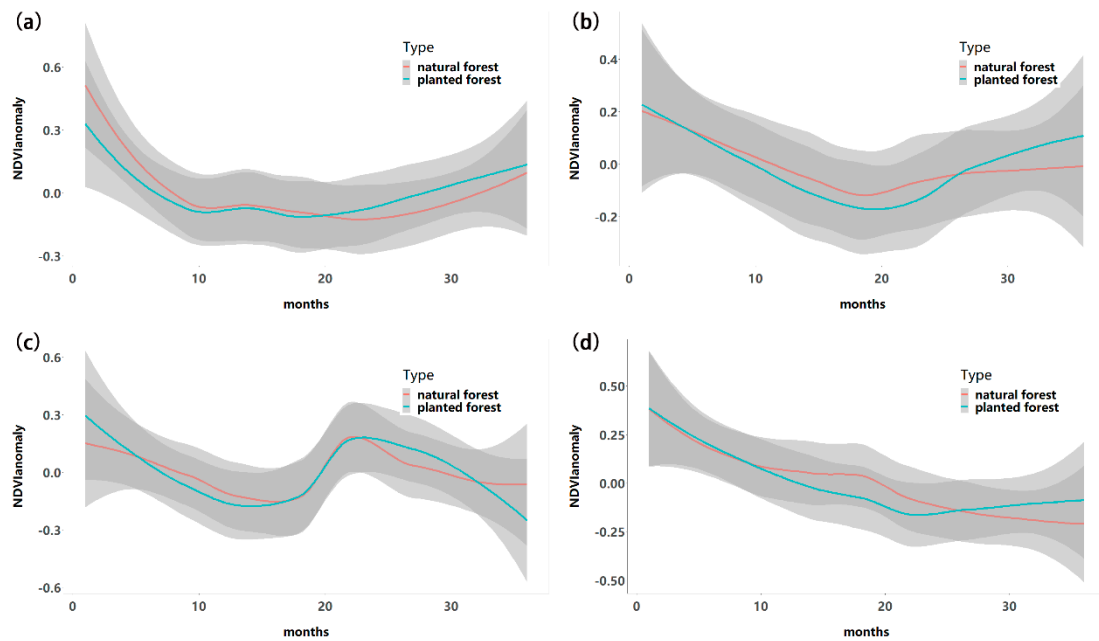


Figure A4. Seasonal changes in the index of $NDVI_{anomaly}$ after all drought events: (a) Spring; (b) Summer; (c) Autumn; (d) Winter. The solid lines denote mean values of $NDVI_{anomaly}$. The gray shadows denote standard deviation of $NDVI_{anomaly}$.

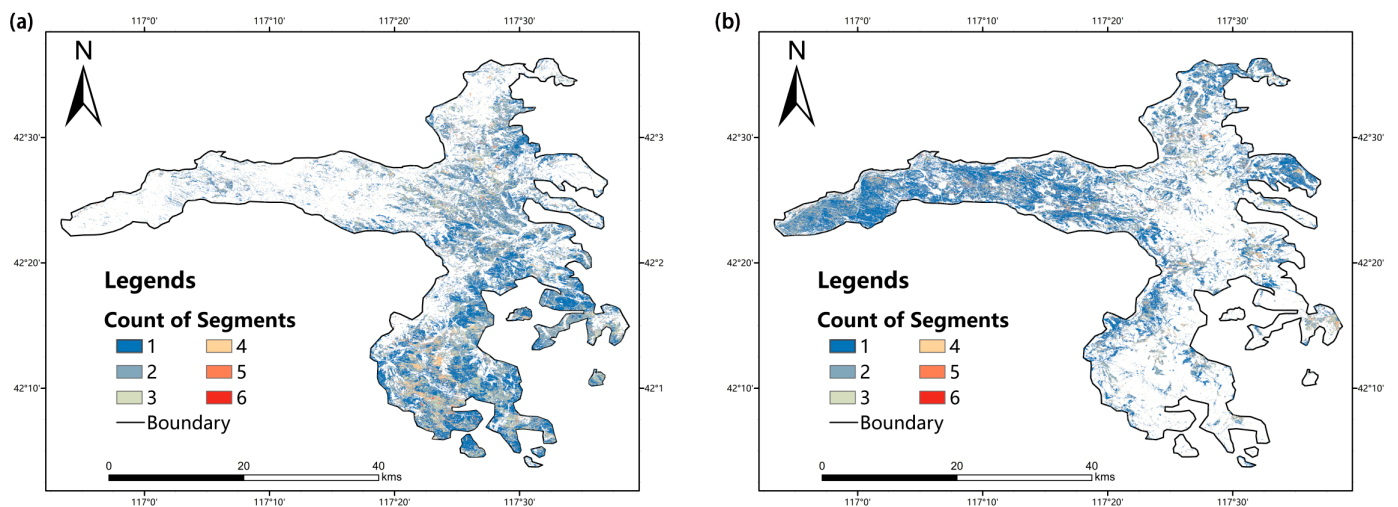


Figure A5. The number of segments detected in every pixel of planted (a) and natural (b) forests during the period from 1985 to 2020 in the Saihanba region.

References

1. FAO. *Global Forest Resources Assessment 2020: Main Report*; FAO: Rome, Italy, 2020.
2. Bonan, G.B. Forests and Climate Change: Forcings, Feedbacks, and the Climate Benefits of Forests. *Science* **2008**, *320*, 1444–1449. [[CrossRef](#)]
3. Seidl, R.; Thom, D.; Kautz, M.; Martin-Benito, D.; Peltoniemi, M.; Vacchiano, G.; Wild, J.; Ascoli, D.; Petr, M.; Honkaniemi, J.; et al. Forest disturbances under climate change. *Nat. Clim. Chang.* **2017**, *7*, 395–402. [[CrossRef](#)] [[PubMed](#)]
4. Pickett, S.T.A.; White, P.S. *The Ecology of Natural Disturbance and Patch Dynamics*; Academic Press: New York, NY, USA, 1985.
5. Hansen, M.C.; Potapov, P.V.; Moore, R.; Hancher, M.; Turubanova, S.A.; Tyukavina, A.; Thau, D.; Stehman, S.V.; Goetz, S.J.; Loveland, T.R.; et al. High-Resolution Global Maps of 21st-Century Forest Cover Change. *Science* **2013**, *342*, 850–853. [[CrossRef](#)] [[PubMed](#)]
6. Seidl, R.; Schelhaas, M.-J.; Lexer, M.J. Unraveling the drivers of intensifying forest disturbance regimes in Europe. *Glob. Chang. Biol.* **2011**, *17*, 2842–2852. [[CrossRef](#)]

7. Senf, C.; Seidl, R. Natural disturbances are spatially diverse but temporally synchronized across temperate forest landscapes in Europe. *Glob. Chang. Biol.* **2018**, *24*, 1201–1211. [[CrossRef](#)] [[PubMed](#)]
8. Thom, D.; Rammer, W.; Seidl, R. Disturbances catalyze the adaptation of forest ecosystems to changing climate conditions. *Glob. Chang. Biol.* **2017**, *23*, 269–282. [[CrossRef](#)]
9. Seidl, R.; Fernandes, P.M.; Fonseca, T.F.; Gillet, F.; Jönsson, A.M.; Merganičová, K.; Netherer, S.; Arpacı, A.; Bontemps, J.-D.; Bugmann, H.; et al. Modelling natural disturbances in forest ecosystems: A review. *Ecol. Model.* **2011**, *222*, 903–924. [[CrossRef](#)]
10. Bouchard, M.; Pothier, D. Long-term influence of fire and harvesting on boreal forest age structure and forest composition in eastern Québec. *Forest Ecol. Manag.* **2011**, *261*, 811–820. [[CrossRef](#)]
11. Thom, D.; Seidl, R. Natural disturbance impacts on ecosystem services and biodiversity in temperate and boreal forests. *Biol. Rev. Camb. Philos. Soc.* **2016**, *91*, 760–781. [[CrossRef](#)]
12. Huang, C.; Ling, P.-Y.; Zhu, Z. North Carolina's forest disturbance and timber production assessed using time series Landsat observations. *Int. J. Digit. Earth* **2015**, *8*, 947–969. [[CrossRef](#)]
13. Kasischke, E.S.; Amiro, B.D.; Barger, N.N.; French, N.H.F.; Goetz, S.J.; Grosse, G.; Harmon, M.E.; Hicke, J.A.; Liu, S.; Masek, J.G. Impacts of disturbance on the terrestrial carbon budget of North America. *J. Geophys. Res. Biogeosci.* **2013**, *118*, 303–316. [[CrossRef](#)]
14. Senf, C.; Seidl, R. Mapping the forest disturbance regimes of Europe. *Nat. Sustain.* **2020**, *4*, 63–70. [[CrossRef](#)]
15. Liu, Z.; Wang, W.J.; Ballantyne, A.; He, H.S.; Wang, X.; Liu, S.; Ciais, P.; Wimberly, M.C.; Piao, S.; Yu, K.; et al. Forest disturbance decreased in China from 1986 to 2020 despite regional variations. *Commun. Earth Environ.* **2023**, *4*, 15. [[CrossRef](#)]
16. Hisano, M.; Searle, E.B.; Chen, H.Y.H. Biodiversity as a solution to mitigate climate change impacts on the functioning of forest ecosystems. *Biol. Rev.* **2018**, *93*, 439–456. [[CrossRef](#)]
17. Viljur, M.-L.; Abella, S.R.; Adámek, M.; Alencar, J.B.R.; Barber, N.A.; Beudert, B.; Burkle, L.A.; Cagnolo, L.; Campos, B.R.; Chao, A.; et al. The effect of natural disturbances on forest biodiversity: An ecological synthesis. *Biol. Rev.* **2022**, *97*, 1930–1947. [[CrossRef](#)]
18. Liu, S.; Wu, S.; Wang, H. Managing planted forests for multiple uses under a changing environment in China. *N. Z. J. For. Sci.* **2014**, *44*, S3. [[CrossRef](#)]
19. Feng, X.; Fu, B.; Piao, S.; Wang, S.; Ciais, P.; Zeng, Z.; Lü, Y.; Zeng, Y.; Li, Y.; Jiang, X.; et al. Revegetation in China's Loess Plateau is approaching sustainable water resource limits. *Nat. Clim. Chang.* **2016**, *6*, 1019–1022. [[CrossRef](#)]
20. Hua, F.; Bruijnzeel, L.A.; Meli, P.; Martin, P.A.; Zhang, J.; Nakagawa, S.; Miao, X.; Wang, W.; McEvoy, C.; Peña-Arancibia, J.L.; et al. The biodiversity and ecosystem service contributions and trade-offs of forest restoration approaches. *Science* **2022**, *376*, 839–844. [[CrossRef](#)]
21. Rodríguez-Vallejo, C.; Navarro-Cerrillo, R.M. Contrasting Response to Drought and Climate of Planted and Natural Pinus pinaster Aiton Forests in Southern Spain. *Forests* **2019**, *10*, 603. [[CrossRef](#)]
22. Camarero, J.J.; Gazol, A.; Linares, J.C.; Fajardo, A.; Colangelo, M.; Valeriano, C.; Sanchez-Salguero, R.; Sanguesa-Barreda, G.; Granda, E.; Gimeno, T.E. Differences in temperature sensitivity and drought recovery between natural stands and plantations of conifers are species-specific. *Sci. Total Environ.* **2021**, *796*, 148930. [[CrossRef](#)]
23. Luo, H.; Zhou, T.; Wu, H.; Zhao, X.; Wang, Q.; Gao, S.; Li, Z. Contrasting Responses of Planted and Natural Forests to Drought Intensity in Yunnan, China. *Remote Sens.* **2016**, *8*, 635. [[CrossRef](#)]
24. Tan, Z.-H.; Zhang, Y.-P.; Song, Q.-H.; Liu, W.-J.; Deng, X.-B.; Tang, J.-W.; Deng, Y.; Zhou, W.-J.; Yang, L.-Y.; Yu, G.-R.; et al. Rubber plantations act as water pumps in tropical China. *Geophys. Res. Lett.* **2011**, *38*, L24406. [[CrossRef](#)]
25. Qiu, J. China drought highlights future climate threats. *Nature* **2010**, *465*, 142–143. [[CrossRef](#)] [[PubMed](#)]
26. Barsi, J.A.; Schott, J.R.; Palluconi, F.D.; Helder, D.L.; Hook, S.J.; Markham, B.L.; Chander, G.; O'Donnell, E.M. Landsat TM and ETM+ thermal band calibration. *Can. J. Remote Sens.* **2014**, *29*, 141–153. [[CrossRef](#)]
27. Cao, B.; Yu, L.; Naipal, V.; Ciais, P.; Li, W.; Zhao, Y.; Wei, W.; Chen, D.; Liu, Z.; Gong, P. A 30 m terrace mapping in China using Landsat 8 imagery and digital elevation model based on the Google Earth Engine. *Earth Syst. Sci. Data* **2021**, *13*, 2437–2456. [[CrossRef](#)]
28. Vaglio Laurin, G.; Puletti, N.; Hawthorne, W.; Liesenberg, V.; Corona, P.; Papale, D.; Chen, Q.; Valentini, R. Discrimination of tropical forest types, dominant species, and mapping of functional guilds by hyperspectral and simulated multispectral Sentinel-2 data. *Remote Sens. Environ.* **2016**, *176*, 163–176. [[CrossRef](#)]
29. Gorelick, N.; Hancher, M.; Dixon, M.; Ilyushchenko, S.; Thau, D.; Moore, R. Google Earth Engine: Planetary-scale geospatial analysis for everyone. *Remote Sens. Environ.* **2017**, *202*, 18–27. [[CrossRef](#)]
30. Deines, J.M.; Kendall, A.D.; Crowley, M.A.; Rapp, J.; Cardille, J.A.; Hyndman, D.W. Mapping three decades of annual irrigation across the US High Plains Aquifer using Landsat and Google Earth Engine. *Remote Sens. Environ.* **2019**, *233*, 111400. [[CrossRef](#)]
31. Vicente-Serrano, S.M.; Beguería, S.; López-Moreno, J.I. A Multiscalar Drought Index Sensitive to Global Warming: The Standardized Precipitation Evapotranspiration Index. *J. Clim.* **2010**, *23*, 1696–1718. [[CrossRef](#)]
32. Funk, C.; Peterson, P.; Landsfeld, M.; Pedreros, D.; Verdin, J.; Shukla, S.; Husak, G.; Rowland, J.; Harrison, L.; Hoell, A.; et al. The climate hazards infrared precipitation with stations—A new environmental record for monitoring extremes. *Sci. Data* **2015**, *2*, 150066. [[CrossRef](#)]
33. Muñoz-Sabater, J.; Dutra, E.; Agustí-Panareda, A.; Albergel, C.; Arduini, G.; Balsamo, G.; Boussetta, S.; Choulga, M.; Harrigan, S.; Hersbach, H.; et al. ERA5-Land: A state-of-the-art global reanalysis dataset for land applications. *Earth Syst. Sci. Data* **2021**, *13*, 4349–4383. [[CrossRef](#)]

34. Iverson, L.R.; Graham, R.L.; Cook, E.A. Applications of satellite remote sensing to forested ecosystems. *Landsc. Ecol.* **1989**, *3*, 131–143. [[CrossRef](#)]
35. Xi, Y.; Tian, J.; Jiang, H.; Tian, Q.; Xiang, H.; Xu, N. Mapping tree species in natural and planted forests using Sentinel-2 images. *Remote Sens. Lett.* **2022**, *13*, 544–555. [[CrossRef](#)]
36. Waśniewski, A.; Hościło, A.; Zagajewski, B.; Moukétou-Tarazewicz, D. Assessment of Sentinel-2 Satellite Images and Random Forest Classifier for Rainforest Mapping in Gabon. *Forests* **2020**, *11*, 941. [[CrossRef](#)]
37. Meng, Y.; Wei, C.; Guo, Y.; Tang, Z. A Planted Forest Mapping Method Based on Long-Term Change Trend Features Derived from Dense Landsat Time Series in an Ecological Restoration Region. *Remote Sens.* **2022**, *14*, 961. [[CrossRef](#)]
38. Haralick, R.M. Textural features for image classification. *IEEE Trans. Syst. Man Cybern. SMC* **1973**, *3*, 610–621. [[CrossRef](#)]
39. Farr, T.G.; Rosen, P.A.; Caro, E.; Crippen, R.; Duren, R.; Hensley, S.; Kobrick, M.; Paller, M.; Rodriguez, E.; Roth, L.; et al. The Shuttle Radar Topography Mission. *Rev. Geophys.* **2007**, *45*, RG2004. [[CrossRef](#)]
40. Tucker, C.J. Red and photographic infrared linear combinations for monitoring vegetation. *Remote Sens. Environ.* **1979**, *8*, 127–150. [[CrossRef](#)]
41. McFeeters, S.K. The use of the Normalized Difference Water Index (NDWI) in the delineation of open water features. *Int. J. Remote Sens.* **1996**, *17*, 1425–1432. [[CrossRef](#)]
42. Zha, Y.; Gao, J.; Ni, S. Use of normalized difference built-up index in automatically mapping urban areas from TM imagery. *Int. J. Remote Sens.* **2003**, *24*, 583–594. [[CrossRef](#)]
43. Congalton, R.G. A review of assessing the accuracy of classifications of remotely sensed data. *Remote Sens. Environ.* **1991**, *37*, 35–46. [[CrossRef](#)]
44. Kennedy, R.E.; Yang, Z.; Cohen, W.B. Detecting trends in forest disturbance and recovery using yearly Landsat time series: 1. LandTrendr—Temporal segmentation algorithms. *Remote Sens. Environ.* **2010**, *114*, 2897–2910. [[CrossRef](#)]
45. Pasquarella, V.J.; Arévalo, P.; Bratley, K.H.; Bullock, E.L.; Gorelick, N.; Yang, Z.; Kennedy, R.E. Demystifying LandTrendr and CCDC temporal segmentation. *Int. J. Appl. Earth Obs.* **2022**, *110*, 102806. [[CrossRef](#)]
46. Cohen, W.B.; Yang, Z.; Kennedy, R. Detecting trends in forest disturbance and recovery using yearly Landsat time series: 2. TimeSync—Tools for calibration and validation. *Remote Sens. Environ.* **2010**, *114*, 2911–2924. [[CrossRef](#)]
47. Hislop, S.; Jones, S.; Soto-Berelov, M.; Skidmore, A.; Haywood, A.; Nguyen, T.H. A fusion approach to forest disturbance mapping using time series ensemble techniques. *Remote Sens. Environ.* **2019**, *221*, 188–197. [[CrossRef](#)]
48. Zhou, M.; Li, D.; Liao, K.; Lu, D. Integration of Landsat time-series vegetation indices improves consistency of change detection. *Int. J. Digit. Earth* **2023**, *16*, 1276–1299. [[CrossRef](#)]
49. Wan, L.; Bento, V.A.; Qu, Y.; Qiu, J.; Song, H.; Zhang, R.; Wu, X.; Xu, F.; Lu, J.; Wang, Q. Drought characteristics and dominant factors across China: Insights from high-resolution daily SPEI dataset between 1979 and 2018. *Sci. Total Environ.* **2023**, *901*, 166362. [[CrossRef](#)]
50. Peng, Y.; Peng, T.; Li, Y. Spatiotemporal Characteristics of Drought in Northwest China Based on SPEI Analysis. *Atmosphere* **2023**, *14*, 1188. [[CrossRef](#)]
51. Bae, S.; Lee, S.-H.; Yoo, S.-H.; Kim, T. Analysis of Drought Intensity and Trends Using the Modified SPEI in South Korea from 1981 to 2010. *Water* **2018**, *10*, 327. [[CrossRef](#)]
52. Svoboda, M.D.; Fuchs, B.A. Handbook of drought indicators and indices. In *Drought and Water Crises: Integrating Science, Management, and Policy*, 2nd ed.; World Meteorological Organization: Geneva, Switzerland, 2017.
53. R-Core-Team. R: A Language and Environment for Statistical Computing. 2022. Available online: <https://www.R-project.org/> (accessed on 7 September 2022).
54. Chen, J.; Jönsson, P.; Tamura, M.; Gu, Z.; Matsushita, B.; Eklundh, L. A simple method for reconstructing a high-quality NDVI time-series data set based on the Savitzky–Golay filter. *Remote Sens. Environ.* **2004**, *91*, 332–344. [[CrossRef](#)]
55. Zhong, Z.; He, B.; Chen, Y.; Yuan, W.; Huang, L.; Guo, L.; Zhang, Y.; Xie, X. Higher Sensitivity of Planted Forests’ Productivity Than Natural Forests to Droughts in China. *J. Geophys. Res. Biogeosci.* **2021**, *126*, e2021JG006306. [[CrossRef](#)]
56. Li, L.; Chen, J.; Mu, X.; Li, W.; Yan, G.; Xie, D.; Zhang, W. Quantifying Understory and Overstory Vegetation Cover Using UAV-Based RGB Imagery in Forest Plantation. *Remote Sens.* **2020**, *12*, 298. [[CrossRef](#)]
57. Zhang, X.; Yu, P.; Wang, D.; Xu, Z. Density- and age-dependent influences of droughts and intrinsic water use efficiency on growth in temperate plantations. *Agric. For. Meteorol.* **2022**, *325*, 109134. [[CrossRef](#)]
58. Pawson, S.M.; Brin, A.; Brockerhoff, E.G.; Lamb, D.; Payn, T.W.; Paquette, A.; Parrotta, J.A. Plantation forests, climate change and biodiversity. *Biodivers. Conserv.* **2013**, *22*, 1203–1227. [[CrossRef](#)]
59. Anyamba, A.; Tucker, C.J. Historical perspectives on AVHRR NDVI and vegetation drought monitoring. In *Remote Sensing of Drought: Innovative Monitoring Approaches*, 1st ed.; CRC Press: Boca Raton, FL, USA, 2012.
60. Phillips, O.L.; van der Heijden, G.; Lewis, S.L.; López-González, G.; Aragão, L.E.O.C.; Lloyd, J.; Malhi, Y.; Monteagudo, A.; Almeida, S.; Dávila, E.A.; et al. Drought–mortality relationships for tropical forests. *New Phytol.* **2010**, *187*, 631–646. [[CrossRef](#)] [[PubMed](#)]
61. Guo, Q.; Ren, H. Productivity as related to diversity and age in planted versus natural forests. *Glob. Ecol. Biogeogr.* **2014**, *23*, 1461–1471. [[CrossRef](#)]
62. Yu, Z.; Liu, S.; Wang, J.; Wei, X.; Schuler, J.; Sun, P.; Harper, R.; Zegre, N. Natural forests exhibit higher carbon sequestration and lower water consumption than planted forests in China. *Glob. Chang. Biol.* **2019**, *25*, 68–77. [[CrossRef](#)]

63. Vanhellemont, M.; Sousa-Silva, R.; Maes, S.L.; Van den Bulcke, J.; Hertzog, L.; De Groote, S.R.E.; Van Acker, J.; Bonte, D.; Martel, A.; Lens, L.; et al. Distinct growth responses to drought for oak and beech in temperate mixed forests. *Sci. Total Environ.* **2019**, *650*, 3017–3026. [[CrossRef](#)]
64. Wigneron, J.-P.; Fan, L.; Ciais, P.; Bastos, A.; Brandt, M.; Chave, J.; Saatchi, S.; Baccini, A.; Fensholt, R. Tropical forests did not recover from the strong 2015–2016 El Niño event. *Sci. Adv.* **2020**, *6*, eaay4603. [[CrossRef](#)]
65. Choat, B.; Brodribb, T.J.; Brodersen, C.R.; Duursma, R.A.; López, R.; Medlyn, B.E. Triggers of tree mortality under drought. *Nature* **2018**, *558*, 531–539. [[CrossRef](#)]
66. Li, X.; Piao, S.; Huntingford, C.; Peñuelas, J.; Yang, H.; Xu, H.; Chen, A.; Friedlingstein, P.; Keenan, T.F.; Sitch, S.; et al. Global variations in critical drought thresholds that impact vegetation. *Natl. Sci. Rev.* **2023**, *10*, nwad049. [[CrossRef](#)] [[PubMed](#)]
67. Yaseef, N.R.; Yakir, D.; Rotenberg, E.; Schiller, G.; Cohen, S. Ecohydrology of a semi-arid forest: Partitioning among water balance components and its implications for predicted precipitation changes. *Ecohydrology* **2010**, *3*, 143–154. [[CrossRef](#)]
68. Anderegg, W.R.L.; Trugman, A.T.; Badgley, G.; Konings, A.G.; Shaw, J. Divergent forest sensitivity to repeated extreme droughts. *Nat. Clim. Chang.* **2020**, *10*, 1091–1095. [[CrossRef](#)]
69. Chen, H.Y.H.; Luo, Y. Net aboveground biomass declines of four major forest types with forest ageing and climate change in western Canada's boreal forests. *Glob. Chang. Biol.* **2015**, *21*, 3675–3684. [[CrossRef](#)]

Disclaimer/Publisher's Note: The statements, opinions and data contained in all publications are solely those of the individual author(s) and contributor(s) and not of MDPI and/or the editor(s). MDPI and/or the editor(s) disclaim responsibility for any injury to people or property resulting from any ideas, methods, instructions or products referred to in the content.